On the SERS quantitative determination of organic dyes

On the SERS quantitative determination of organic dyes

Marilena Ricci, Elisa Trombetta, Emilio Castellucci [#] and Maurizio Becucci [#1]

Department of Chemistry 'Ugo Schiff', University of Florence, via della Lastruccia 3-13, 50019 Sesto Fiorentino (FI), Italy

[#]also at LENS, University of Florence, via N. Carrara 1, 50019 Sesto Fiorentino (FI), Italy

Abstract

The use of SERS methods for the quantitative determination of different molecular species is not trivial as many parameters seriously affect the outcome of any experiment. In this work, we use as a case study the quantitative analysis of ionic organics dyes. We report on the role of different molecular properties to the modulation of the SERS signal, the useful dynamic range for the determination, the dynamics of the molecule-nanoparticle interaction process and the time dependency of the signal. The consequences on the quantitative determination on dye mixtures, often found in the analysis of artworks, are discussed.

Keywords: SERS; alizarin; carminic acid; rhodamine 6G; safranin

[1] corresponding author: maurizio.becucci@unifi.it

Introduction

Since early times, the capabilities of SERS (Surface Enhanced Raman Scattering) for the identification of organic molecules in low concentration in solution have been assessed. Different reports have shown the possibility to detect signals originating from a single molecule absorbed on the surface of a metal (Ag or Au, typically) cluster of nanometric dimensions (NP).[1-3] Towards this goal, the relevance of many features both of the metal nanoparticles and the analyte have been highlighted and discussed.[3-9] The possible application of SERS methods for the identification of organic dyes present in works of art, textile fibers and other materials has been presented and reviewed.[10-13] More critical is the possibility to obtain a quantitative determination of the analyte by SERS techniques because many parameters strongly affect the measured signal and the need of standard solution for calibration.[14]

SERS experiments provide a much higher sensitivity than the conventional Raman ones due to a number of factors. The Raman effect is classically described as the generation of new frequencies in the radiation scattered by a molecular system when it is excited by monochromatic radiation. This process is related to the polarizability of the molecule (or, more precisely, to its variation with molecular vibrations in case of vibrational Raman scattering experiments) and the intensity of the field interacting with the molecule. If a molecule is adsorbed on the surface of a metal particle of nanometric dimensions (NP), it can be subject to a Raman scattering process with peculiar properties.[15,16] The electrons in the Fermi levels on the surface of the metal NP can be driven in a true collective oscillatory motion (the “surface plasmon”) by an external EM field. The plasmon resonance frequency is controlled both by the nature of the metal involved and by the NP physical dimensions. A molecule absorbed on the NP surface that is excited in its plasmonic resonance can experience a very strong local field, which can lead to an anomalously strong Raman scattering process. Classical electrodynamics calculation can show that if two metal NPs are very close, when

they are excited in the plasmonic resonance, the electric field in the gap between them is extremely high.[17] Then, if a molecule is placed in this gap an extremely strong Raman signal can be obtained.[1,5] Similar local conditions are referred as “hot spots” in SERS experiments. Furthermore, chemical processes can modulate the vibrational contributions to polarizability of the molecule that are responsible of the Raman scattering process. The formation of a chemical bond between the absorbed molecule and the nanoparticle represents a major modification of the local polarizability of the system. In a SERS experiment the vibrational bands more directly related to local vibrations involving the atoms bonded to the cluster are most affected by the signal enhancement. Therefore, both chemical and physical effects are relevant for the SERS process.[4,7,9] Other experimental factors can be relevant, as well. Very important is the closeness of the molecular electronic transitions to the excitation frequency, exactly as it is occurring in case of the ordinary Resonance Raman experiments. However, more subtle effects can occur in case of SERS, such as the possible occurrence of charge-transfer (CT) molecule↔cluster electronic transitions. These processes gain efficiency in SERS with both their closeness to resonance (with respect to the excitation frequency) and cross-section.

SERS has been used for the identification of organic dyes present in different materials.[18-20] Its use was extremely valuable for applications in the field of cultural heritage studies and conservation.[10,13,18,21-23] It offers the possibility to identify these materials without detriment of these unique samples, with no need of destructive sampling or complex analytical methods. Recent developments have shown the possibility of local micro-extraction of the dyes on inert substrates (solvent assisted), followed by addition of metal nanoparticles to the substrate and then SERS analysis.[11,24-26] The identification of the dye present in the sample is possible thanks to the high molecular specificity of the SERS signal. A possible problem arises when dealing with samples tinted

with natural dyes. Natural products, such as those obtained by the madder (Rubia Tinctorum) roots are a mixture of hydroxyanthraquinonic dyes, such as 1,2-dihydroxyanthraquinone (alizarin), 1,3-dihydroxyanthraquinone (purpuroxanthin), 1,4-dihydroxyanthraquinone (quinizarin) and 1,2,4-trihydroxyanthraquinone (purpurin). Carminic acid, another natural dye obtained from insects, contains the same anthraquinonic chromophore. The identification and quantification of the different components can be useful for understanding both the preparation of the sample and its geographical origin.[27] At present, chromatographic methods are used for this kind of determination but a tedious preparation of the sample is needed and the analysis is destructive.[27-29] Most recently, a few publications have introduced the possibility of SERS use for this purpose and properties of binary or more complex dye mixtures have been investigated.[30-32] Despite the very similar Raman cross sections of the different dyes (in non-resonant conditions), they have much different enhancement of signals in SERS. This represents a possible limitation for the general applicability of this method.

This work aims to highlight a few fundamental points relevant for the determination of dyes content by SERS spectroscopic methods. We will focus on the nature of the molecule-substrate interaction, and on the problems possibly arising for the quantification of dyes absorbed on metal nanoparticles. We have experimentally studied the SERS signals obtained preparing colloidal dispersions of silver nanoparticles (AgNPs) with different concentration of ordinary organic dyes. We have selected two anthraquinonic dyes, alizarin (Az) and carminic acid (CA), which in water can exist in different neutral or ionic forms (corresponding to different colors).[33-35] We investigated two cationic dyes as well: Rhodamine 6G (R6G) and Safranin (SA). R6G is one of the most used dyes for fundamental SERS studies and its Raman spectrum is well known.[36-38] SA is a cationic dye, related to aniline, widely used as a biological stain. In the early times of cinematography, it was used for toning of black and

white films. SA vibrational properties have been extensively studied.[39,40] A sketch of the different molecular structures is shown in Fig. 1.

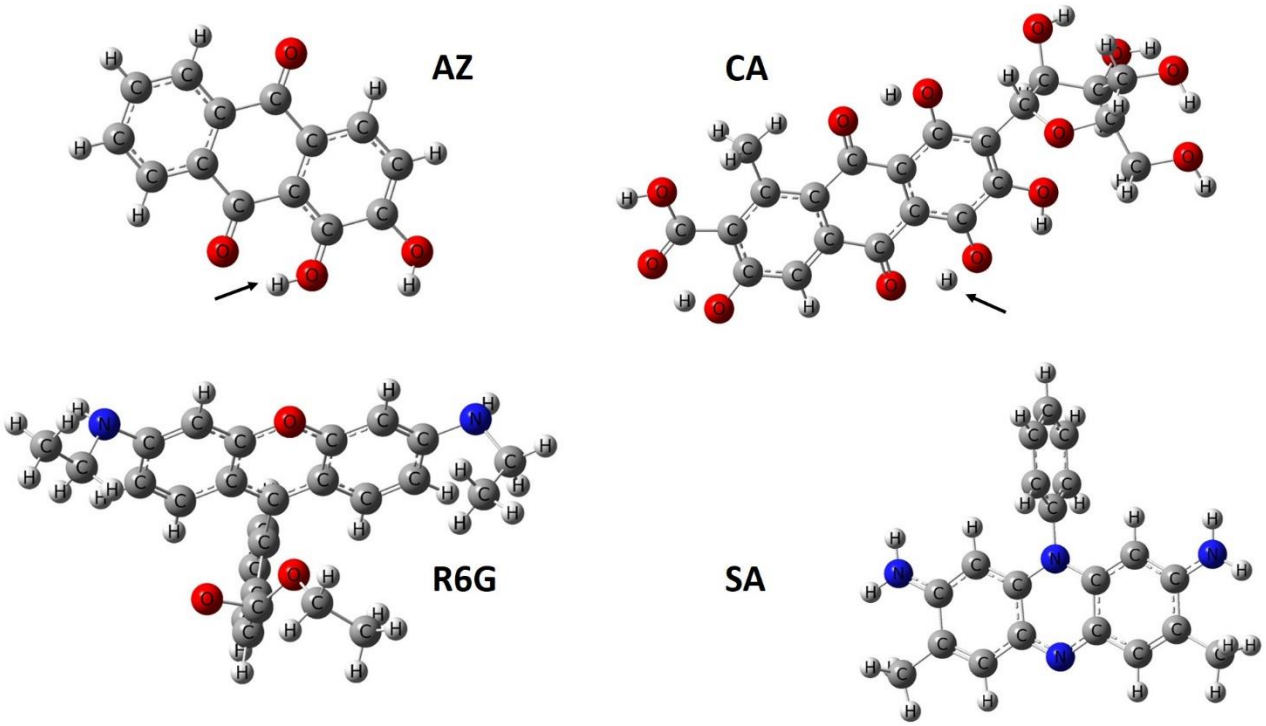

Figure 1. The structure of the dyes used in this study. The arrows point to the hydroxyl group in involved in Az anion and CA di-anion formation.

Experimental

The colloidal dispersion of silver nanoparticles was prepared according to the traditional Lee-Meisel procedure[41], by reduction of silver nitrate with trisodium citrate dihydrate. In particular, after a reduction time of 60 min, the flask containing the colloidal solution was placed in an ice bath to cool. This prompt cooling process of the colloidal dispersion has been adopted in order to obtain a narrow distribution of nanoparticle sizes having an average diameter of about 40 nm.

The temporal stability of the AgNPs was checked by the measure of their visible extinction spectrum and the determination of the frequency, intensity and spectral width of the plasmonic band.

Alizarin and carminic acid were studied in water solution at pH 8 where the dominant species are their monoanion (AzA) and di-anion (CA), respectively.[35,41-44] The cationic dyes exist in a single ionic form: it was then possible to work in water or native colloidal dispersions. All the different dyes under study exhibit strong HOMO-LUMO transition in the spectral region 500-550 nm, in the selected pH ranges.

The samples were prepared by adding 0.5 ml of water (or 10^{-2} M phosphate buffer at pH=8.0) to 0.5 ml of the colloidal dispersion in a 1 cm optical path-length quartz cuvette, continuously stirred with a small magnetic bar. Then, a small volume of the 10^{-3} or 10^{-4} M dye solution was added in order to reach dye analytical concentration from 10^{-4} to 10^{-7} M and the sample let to equilibrate for 20 minutes, unless differently specified. This time delay between the sample preparation and the measure of the SERS spectrum was chosen, after a few initial tests, in order to have good signals and reproducible conditions. Each measurement for the different datasets was carried out with AgNPs from the same batch of synthesis. Repeated measurements with AgNPs from different batch of synthesis were providing the same kind of results for the different datasets.

Raman spectra were measured with a Raman spectrometer based on an Acton SP150 monochromator, equipped with 600 or 1200 lines/mm holographic gratings, and a Princeton Instruments Pixis CCD detector thermoelectrically cooled. Different lasers were aligned to the spectrometer (785 nm diode laser, 632.8nm He-Ne laser, and 514.5 nm Ar laser) and holographic notch filters (OD 4-6) were used for rejection of the elastically scattered radiation. We used the 785 nm laser line and the full 200-3000 cm^{-1} spectrum was measured in a single acquisition on the CCD camera with the 600 lines/mm grating. The spectral resolution (FWHM of narrow bands) was around 10 cm^{-1}, corresponding to 3 pixels in the CCD camera. Typical laser power on the sample was 5 mW, to avoid strong laser induced effects, and the laser beam was blocked when measurements were

not running. Typical acquisition times were 10-30 s. All the spectra we compare as a function of different parameters are normalized by laser power and integration time.

The selected excitation wavelength (785 nm) allows us to work in pre-resonant conditions equivalent for the different dyes, as we excite the molecules more than 0.5eV far from their HOMO-LUMO resonance.

Results and Discussion

We operate in two steps to demonstrate the dependency of the SERS signal to the dye concentration. At first, we measured the SERS signal as a function of the analytical concentration of the dye in the samples. Then, we measured the Raman spectrum of the same dye in a solution of suitable concentration and we calculated the SERS analytical enhancement factor[3] according to the formula

$$\text{SERS analytical enhancement factor} = \frac{I_{SERS}}{n_{SERS}} \frac{n_{Raman}}{I_{Raman}}$$

where the observed SERS and Raman intensities (I) are divided by the analytical dye concentration in the corresponding samples (n).

To work with anthraquinonic dyes in pH 8 solution we used a phosphate buffer to set and stabilize the pH value and we added to the colloidal dispersion in use an equal volume of buffered solution before the addition of the dye (already dissolved in the buffered solution). The properties of the colloidal dispersion are possibly affected by the changes in pH and solution ionic strength. In the Supplementary Information (Figure S1) we report the extinction spectrum of the colloidal dispersion in the different experimental conditions and its stability over time.

In Figure 2 we show typical AzA SERS spectra measured in pH 8 buffered solutions. The two peaks around 1000 cm^{-1}, due to the presence of phosphate anions,[45] are clearly observed in the blank (colloidal dispersion + phosphate buffer) and in the more diluted AzA samples. In the left panel the extended spectrum is shown, including the broad band above 3000 cm^{-1}, due to the OH stretching modes of water. The uniform intensities in the different spectra of these bands associated to water is a demonstration of the effectiveness of our data normalization process.

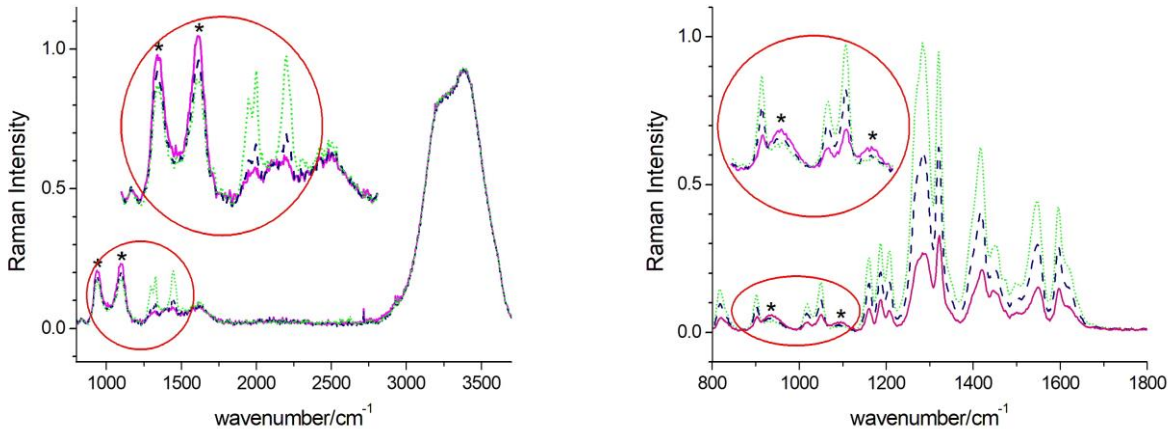

Figure 2. The AzA SERS spectra (background subtracted and normalized to the overall maximum signal) of solutions with different dye analytical concentration. Left panel: AzA concentration 0.1, 0.3 and 0.75 μM (solid, dash and dot lines, respectively). Right panel: AzA concentration 10, 40, 80 μM (solid, dash and dot lines, respectively). The insets show in details the phosphate bands (marked) and selected AzA bands.

The different bands in the AzA SERS spectrum change uniformly as a function of the analytical dye concentration. As an example, we report in Figure 3 results obtained for the 1322 cm^{-1} band: the set of peak intensities (from spectra already normalized for laser power and integration time) obtained on the different samples is further arranged in a relative scale to the maximum observed signal. This 1322 cm^{-1} band is one of the strongest in the AzA SERS spectrum: it is assigned to a combination of CC stretching and CCH bending modes of the anthraquinonic system.[35] The change of this signal with dye concentration is rather complex, revealing different regimes for the SERS mechanism. Further insight on the nature of the process can be gained by looking at the

enhancement factor. The SERS analytical enhancement factor is determined as described above, taking as the reference Raman spectrum obtained on the 10^{-2} M dye solution. The determined values of the AzA SERS enhancement factors as a function of the dye concentration are shown in Figure 3 on the right panel. It is quite evident that for the lowest values of concentration (below 1 μM) the enhancement factor is extremely high and it is falling down very rapidly (by more than one order of magnitude) for larger dye concentration. The enhancement factor is higher than $5*10^5$ at concentration 100 nM and it is around $5*10^4$ for concentration 10 μM.

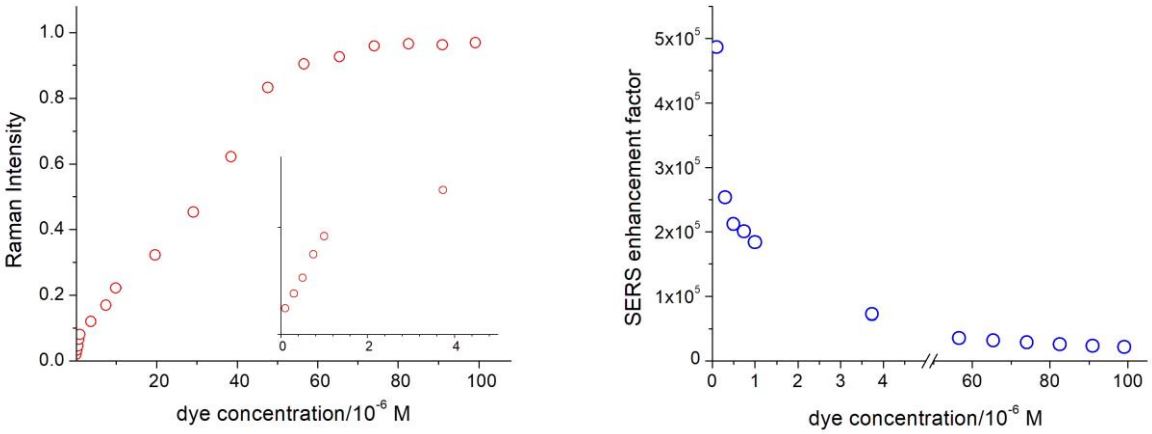

Figure 3. The AzA SERS signal (normalized for laser power and integration time, left panel) and the corresponding analytical enhancement factor (right panel) are plotted as a function of the dye concentration in solution. The inset in the left panel shows the detail of the plot for low dye concentration.

These data, together with simple chemical modeling, suggest a rather simple description of the system. Recent work has shown that alizarin anion binds directly to the AgNPs surface with its oxygen atoms that are evidenced by the arrow in Fig. 1.[42,43] A reasonable estimation of the nanoparticles concentration in the colloidal solutions can be obtained by the measurement of the sample extinction spectrum.[46] The position of the extinction maximum we observe in the native colloidal dispersion is 415nm, corresponding to a most probable NPs diameter of 45 nm. Similar particles have a typical extinction factor $\epsilon = 3*10^{10}$ L mol^{-1} cm^{-1} thus, for a measured absorbance

A=2.0 on an optical path-length of 2mm, the AgNPs concentration is approximately 2.5* 10^{-10} M. The area of a single AZ molecule, in the reported interaction geometry[42], is 7*10^{-1} nm^2, according to simple molecular modeling. Then, the coverage with a continuous monolayer should be obtained with an analytical dye concentration of 1.5*10^{-6} M. Figure 3 shows that AzA has the strongest SERS enhancement factor at concentration below 10^{-6} M. This value is consistent with the maximum number of AzA needed for the monolayer formation on the surface of the AgNPs, as calculated with our very simple model. The strong enhancement factor for molecules absorbed in the first monolayer can be interpreted as the consequence of their chemical interaction with the NPs and exposition to the strongest electric field due to the plasmonic excitation on the metal surface, too. At higher AzA nominal concentration probably the molecules are adsorbed in external layers and the corresponding Raman enhancement factor is decreasing progressively.[5] We did not try to model the system with other methods, either computational or experimental, but our hypothesis is supported also by a careful examination of the SERS spectra for different AzA concentrations. Phosphate ions are known to chemically interact with Ag NPs and to form a monolayer coverage.[45,47] Also, they give rise to weak SERS bands around 950 and 1080 cm^{-1}.[45] For instance, methods have been devised to sensitively detect phosphates in SERS “turn-off” experiments by looking on a sensor at the quenching of the SERS signal of a reporting molecule.[47] The two phosphate bands, even if weak, are present in the Raman spectrum of the buffered colloidal solution and their intensity decreases with the increase in AzA content. Their decrease is quite strong for low dye concentration and continues, at lower rate, for high dye concentrations. This suggests that AzA is able to interact strongly with the AgNPs surface and to replace the phosphate ions initially bound. Figure 2 shows the relative change of the phosphate and AzA bands in SERS spectra at different dye analytical concentrations.

SERS spectra of the CA in solution, either as single dye or as a component of a binary dye mixture are well known.[33,44,48] Also, it was reported a much lower sensitivity for its detection by SERS with respect to alizarin. CA is an acid much stronger than Az.[34] The carboxylic function ionizes already around pH 3. In solution at pH 8 CA forms a di-anion by deprotonation of the same hydroxyl function involved in the Az first deprotonation step.[42,44] SERS spectra at different concentration in the pH=8 phosphate buffered solution reveal that even at high CA concentration the phosphate bands are still evident, in contrast to the AzA case (see Figure 4). These evidences suggest that CA is not efficiently interacting with the AgNPs in our experimental conditions. A CA SERS spectrum in solution with reasonable S/N ratio is obtained only for analytical dye concentration well above 100 μM, almost two orders of magnitude above in the AzA case.

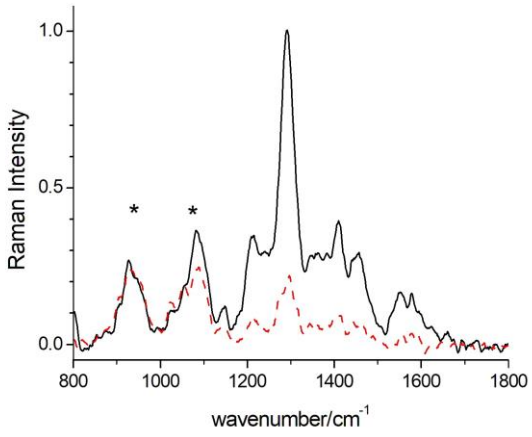

Figure 4. The SERS spectra of CA dianion in pH 8 buffered solution ($2x10^{-4}$ M and 10^{-3} M datasets are plotted as dashed and continuous lines, respectively; baseline subtracted only, marks indicate the phosphate ions bands).

Completely different is the situation occurring for SERS experiments on cationic dyes. SERS spectra of both SA and R6G were already characterized.[39,49] We focus the following discussion on the changes of the representative SERS peak for SA and R6G at 615 and 1365 cm^{-1}, respectively. The results we obtained at first on SA reveal a peak for the SERS signal (Figure 5, left) and an analytical enhancement factor of $\backsim 2.2*10^5$ at 2.5 μM dye concentration, followed by a long tail of weaker

signals at higher concentrations. This kind of behavior was quite surprising, at a first glance, so that we repeat the measurement using R6G, one of the dyes most used for testing the SERS effect. The results were very similar, with a SERS signal peak at 20 μM R6G analytical dye concentration (Figure 5, right).

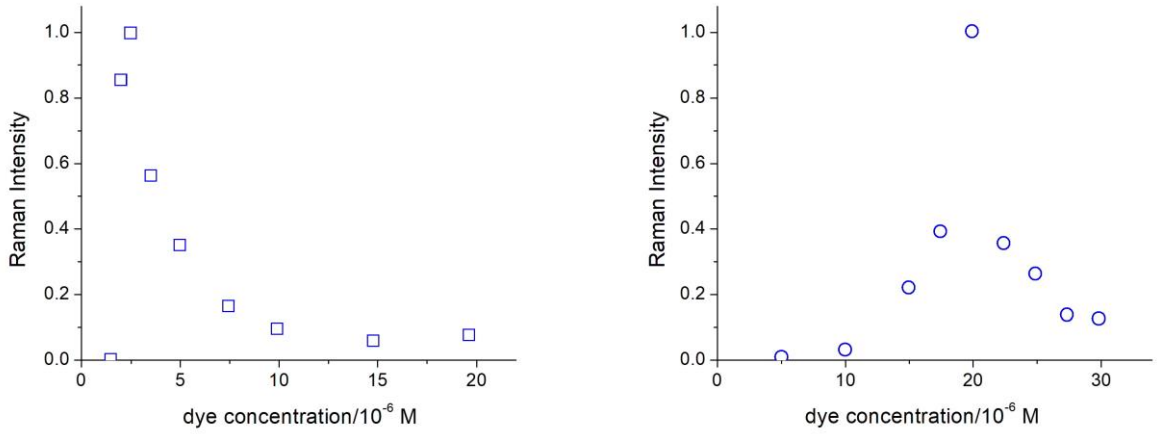

Figure 5. The SA (left) and R6G (right) SERS relative intensities (normalized for laser power and integration time, left panel) as a function of the dye concentration in solution.

A complementary information that helps to understand the present results comes from the analysis of the SERS signal time-dependency (delay between sample preparation and Raman measurement) for different dye concentrations. This time-dependency is not always presenting the same trend for our dye solutions. The most peculiar features are shown by the cationic dyes. In case of anionic dyes, for different concentrations, the SERS signal is increasing with the delay time after sample preparation, at least in the 30 minutes time window we investigated. The results we obtained for AzA are reported in Figure 6 (left). Instead, cationic dyes show a complex dependency on both time-delay and dye concentration (see results on SA in Figure 6, right). For low dye concentration the signal raises up in the first 2-3 minutes and then keep growing at a much slower rate. For high concentrations, the signal has a strong surge in the first 2 minutes and then it falls steadily.

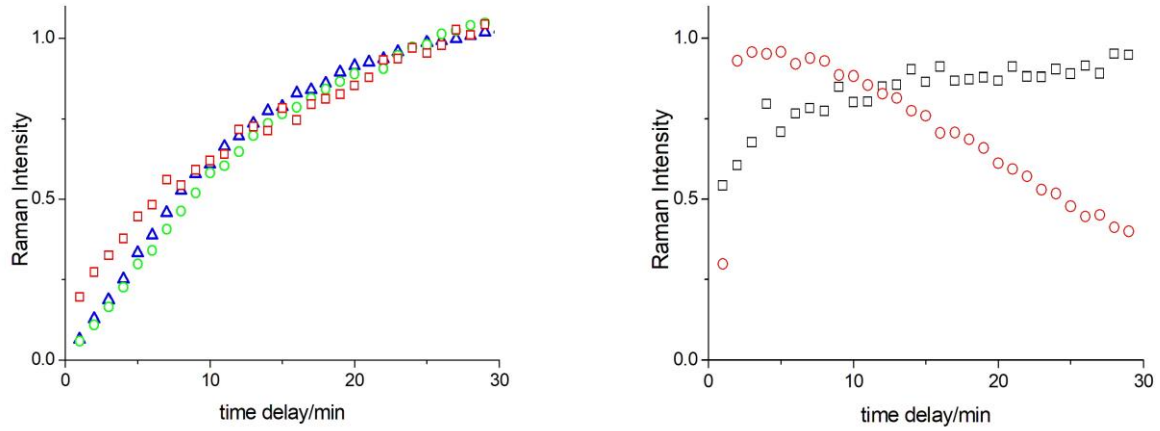

Figure 6. The SERS signals as a function of the delay between sample preparation and measurement for AzA (left) and SA (right) solutions at different analytical concentration. AzA: squares, circles and triangles for 1, 20 and 80 μM dye concentration, respectively. SA: squares and circles for 1.5 and 3.0 μM dye concentration, respectively (the maximum SERS efficiency occurs for dye concentration 2-2.5 μM).

These results can find a rational explanation taking into account the details of the molecule/nanoparticle interaction. The AgNPs formed with the Lee-Meisel synthesis method are stabilized by electrostatic interactions as the citrate anion, used for Ag^+ chemical reduction, is in excess and it binds to the AgNPs surface.[41] Then the phosphate ions, that are present in the buffer solution we used to set a higher pH value, replace the citrate in the first monolayer and induce AgNPs aggregation. AzA has a stronger affinity to the AgNPs surface and replaces the phosphate ions, as can be deduced looking at the simultaneous change of the AzA and phosphate band in the SERS spectra as a function of the Az concentration, as shown in Fig. 2. The time evolution of the SERS signal depends only on the rate of this substitution process and it shows a common trend for the different alizarin concentrations.

Quite different is the mechanism of interaction for the cationic dyes with the AgNPs. The cations do not bind directly the metal surface but they can electrostatically interact with the negative citrate ions present on the metal surface. This process reduces the repulsion between different AgNPs and can promote NPs aggregation (and possibly flocculation).[50] If the AgNPs aggregate they will become

much closer one to the other: the electric field resulting from surface plasmonic excitation is strongly distorted. It is known that in the gap between close particles the field is higher by orders of magnitude with respect to the one of around an isolated NP and the plasmonic resonance frequency shifts to the red. In the field of SERS, similar arrangements are called “hot spots” to indicate that these are singularities where the efficiency of the SERS effect is extremely high. If a similar mechanism is acting in our systems, it would result in a strong, non-linear increase of the SERS signal with the increase of the cationic dye concentration: the signal will raise both because of the increase of the dye concentration and because of the hot-spot creation. At higher dye concentration, the SERS signal should drop: the AgNPs continue to aggregate until flocculation occur and, then, these large aggregates will separate from the solution, leaving the volume probed by the experiment. This mechanism could explain also the time behavior observed in the experiments with cationic dyes where, possibly, the signal changes with a time constant related to the diffusion of the AgNPs. At low values of dye concentration, an increase in size of the metal clusters by aggregation results in a larger signal. At higher values, flocculation is occurring due to the larger number of positively charged particles: after a very rapid formation of small clusters, their excessive growth will make them unstable and flocculation will remove sample from the experimental volume.

The full set of our data suggests that the presence of large substituents on the chromophore skeleton of the dye limits the enhancement of the Raman signal in presence of metal nanoparticles. In case of anionic dyes, we observe a much higher sensitivity for AzA than for CA detection, even if the two molecules differ only for the presence of an OH group and a glycoside ring on the anthraquinonic system. The difference in detection limit by SERS corresponds to the different affinity of the dye to the metal surface, as shown by their different capability to displace the phosphate ions from the metal surface. The problem needs further investigation, possibly by

adequate theoretical modeling including the presence of both many adsorbed molecules and solvent. However, the key factor seems to be the different affinity to the metal surface of the two dyes and the steric interactions that limit the effective metal coverage by the larger dye. In case of the cationic dyes Rh6G and SA, the positive charge is localized between the conjugated system and its amino substituents[39,51] and it is much less accessible in the case of R6G due to the presence of flexible chains (see Figure 1). The lower R6G efficiency in NPs flocculation leads to higher nominal dye concentration at which the maximum SERS signal is observed: 3 and 20 μM for SA and R6G, respectively.

Conclusions

We have shown that different classes of dyes possibly give a strong SERS signal when interaction with AgNPs in solution occurs. However, many details in the interaction mechanism possibly modulate the efficiency of this process: that strongly limits the general application of SERS methods as a simple experiment for high sensitivity quantification of these materials. The change of SERS signal with dye nominal concentration in solution is strongly non-linear and, possibly, its trend in not monotonous. In the case of anionic dyes, we recognize different conditions as a function of the dye concentration and their molecular structures. In favorable cases, at lower concentrations (up to ~1μM) the dye binds to the metal surface to form a monolayer and the SERS enhancement process is very effective. At intermediate concentrations, higher order coverage is possible and the SERS efficiency decreases for these molecules not directly bound to the metal surface, up to a negligible enhancement and an effective saturation of the SERS signal. A calibration of the signal is possible and quantitative experiments can be performed up to the saturation regime. If the dye interaction with the NPs is not strong, the SERS enhancement factor is much smaller and the useful regime of response is correspondingly reduced. Therefore, the relative sensibility of the method changes

strongly for the different dyes according to their specific interaction mechanism with the metal surface. In case of dye mixtures, in order to have a reliable quantitative measurements, experiments must be done for dye concentrations below the threshold for monolayer formation, otherwise competition in the binding process with the metal surface must be taken into account together with the change in SERS efficiency with the different adsorption regime. The situation is much more complex for cation dyes as a quantitative determination is possible only up to the nominal concentration corresponding to the maximum SERS signal. The strong non-linear behavior of the signal with the dye concentration reduce severely the useful measurable range of concentrations.

Acknowledgments

Financial support from Fondazione Cassa di Risparmio di Firenze (project nr. 2016/13363) is gratefully acknowledged.

References

[1] K. Kneipp, Y. Wang, H. Kneipp, L.T. Perelman, I. Itzkan, R.R. Dasari, et al., *Phys. Rev. Lett.*, **1997**, *78*, 1667.

[2] E.C. Le Ru, P.G. Etchegoin, M. Meyer, *J. Chem. Phys.*, **2006**, *125*, 164705.

[3] E.C. Le Ru, E. Blackie, M. Meyer, P.G. Etchegoin, *J. Phys. Chem. C*, **2007**, *111*, 13794.

[4] J.R. Lombardi, R.L. Birke, *J. Phys. Chem. C*, **2008**, *112*, 5605.

[5] E.C. Le Ru, P.G. Etchegoin, *Principles of Surface Enhanced Raman Spectroscopy*, Elsevier: 2009.

[6] A. Zoppi, S. Trigari, G. Margheri, M. Muniz-Miranda, E. Giorgetti, *RSC Adv.*, **2015**, *5*, 8523.

[7] D.L. Jeanmaire, R.P. Van Duyne, *J. Electroanal. Chem. Interfacial Electrochem.*, **1977**, *84*, 1.

[8] M. Fleischmann, P.J. Hendra, A.J. McQuillan, *Chem. Phys. Lett.*, **1974**, *26*, 163.

[9] M.G. Albrecht, J.A. Creighton, *J. Am. Chem. Soc.*, **1977**, *99*, 5215.

[10] M. Leona, *Proc. Natl. Acad. Sci. U. S. A.*, **2009**, *106*, 14757.

[11] C. Lofrumento, M. Ricci, E. Platania, M. Becucci, E. Castellucci, *J. Raman Spectrosc.*, **2013**, *44*, 47.

[12] E. Platania, C. Lofrumento, E. Lottini, E. Azzaro, M. Ricci, M. Becucci, *Anal. Bioanal. Chem.*, **2015**, *407*, 6505.

[13] M. Ricci, C. Lofrumento, E.M. Castellucci, M. Becucci, *J. Spectrosc.*, **2016**, *2016*, 1380105.

[14] I.T. Shadi, B.Z. Chowdhry, M.J. Snowden, R. Withnall, *Spectrochim. Acta Part A Mol. Biomol. Spectrosc.*, **2003**, *59*, 2213.

[15] P. Etchegoin, L.F. Cohen, H. Hartigan, R.J.C. Brown, M.J.T. Milton, J.C. Gallop, *J. Chem. Phys.*, **2003**, *119*, 5281.

[16] K.A. Willets, R.P. Van Duyne, *Annu. Rev. Phys. Chem.*, **2007**, *58*, 267.

[17] S. Y. Huang, B.I. Wu, S. Foong, *J. Appl. Phys.*, **2013**, *113*, 44304.

[18] F. Casadio, M. Leona, J.R. Lombardi, R. Van Duyne, *Acc. Chem. Res.*, **2010**, *43*, 782.

[19] C. Muehlethaler, M. Leona, J.R. Lombardi, *Anal. Chem.*, **2015**, *88*, 152.

[20] E. Platania, J.R. Lombardi, M. Leona, N. Shibayama, C. Lofrumento, M. Ricci, *et al*., *J. Raman Spectrosc.*, **2014**, *45*, 1133.

[21] F. Pozzi, M. Leona, *J. Raman Spectrosc.*, **2016**, *47*, 67.

[22] S. Bruni, V. Guglielmi, F. Pozzi, *J. Raman Spectrosc.*, **2011**, *42*, 1267.

[23] K.L. Wustholz, C.L. Brosseau, F. Casadio, R.P. Van Duyne, *Phys. Chem. Chem. Phys.*, **2009**, *11*, 7350.

[24] B. Doherty, B.G. Brunetti, A. Sgamellotti, C. Miliani, , *J. Raman Spectrosc.*, **2011**, *42*, 1932.

[25] B. Doherty, F. Presciutti, A. Sgamellotti, B.G. Brunetti, C. Miliani, *J. Raman Spectrosc.*, **2014**, *45*, 1153.

[26] M. Leona, J. Stenger, E. Ferloni, *J. Raman Spectrosc.*, **2006**, *37*, 981.

[27] M. Puchalska, K. Połeć-Pawlak, I. Zadrożna, H. Hryszko, M. Jarosz, *J. Mass Spectrom.*, **2004**, *39*, 1441.

[28] M.P. Colombini, A. Andreotti, I. Bonaduce, F. Modugno, E. Ribechini, *Acc. Chem. Res.*, **2010**, *43*, 715.

[29] I. Degano, E. Ribechini, F. Modugno, M.P. Colombini, *Appl. Spectrosc. Rev.*, **2009**, *44*, 363.

[30] M. Hou, Y. Huang, L. Ma, Z. Zhang, *Nanoscale Res. Lett.*, **2015**, *10*, 437.

[31] F. Pozzi, S. Zaleski, F. Casadio, R.P. Van Duyne, *J. Phys. Chem. C*, **2016**, *120*, 21017.

[32] M.V. Cañamares, D.A. Reagan, J.R. Lombardi, M. Leona, , *J. Raman Spectrosc.*, **2014**, *45*, 1147.

[33] C. Miliani, A. Romani, G. Favaro, *J. Phys. Org. Chem.*, **2000**, *13*, 141.

[34] G. Favaro, C. Miliani, A. Romani, M. Vagnini, *J. Chem. Soc., Perkin Trans.*, **2002**, *2*, 192.

[35] C. Lofrumento, E. Platania, M. Ricci, C. Mulana, M. Becucci, E.M. Castellucci, *J. Mol. Struct.*, **2015**, *1090*, 98.

[36] A.M. Michaels, M. Nirmal, L.E. Brus, *J. Am. Chem. Soc.*, **1999**, *121*, 9932.

[37] N. Leopold, B. Lendl, *J. Phys. Chem. B*, **2003**, *107*, 5723.

[38] L. Jensen, G.C. Schatz, *J. Phys. Chem. A*, **2006**, *110*, 5973.

[39] C. Lofrumento, F. Arci, S. Carlesi, M. Ricci, E. Castellucci, M. Becucci, *Spectrochim. Acta - Part A: Mol. Biomol. Spectrosc.*, **2015**, *137*, 677.

[40] M. Ricci, E. Platania, C. Lofrumento, E.M. Castellucci, M. Becucci, *J. Phys. Chem. A*, **2016**, *120*, 5307.

[41] P.C. Lee, D. Meisel, *J. Phys. Chem.*, **1982**, *86*, 3391.

[42] M.V. Cañamares, J.V. Garcia-Ramos, C. Domingo, S. Sanchez-Cortes, *J. Raman Spectrosc.*, **2004**, *35*, 921.

[43] C. Lofrumento, E. Platania, M. Ricci, M. Becucci, E.M. Castellucci, *J. Phys. Chem. C*, **2016**, *120*, 12234.

[44] M.V. Cañamares, J.V. Garcia-Ramos, C. Domingo, S. Sanchez-Cortes, *Vibr. Spectrosc.*, **2006**, *40*, 161.

[45] G. Niaura, A.K. Gaigalas, V.L. Vilker, *J. Phys. Chem. B*, **1997**, *101*, 9250.

[46] D. Paramelle, A. Sadovoy, S. Gorelik, P. Free, J. Hobley, D.G. Fernig, *Analyst*, **2014**, *139*, 4855.

[47] W. Ji, W. Song, I. Tanabe, Y. Wang, B. Zhao, Y. Ozaki, *Chem. Commun.*, **2015**, *51*, 7641.

[48] A.V. Whitney, F. Casadio, R.P. Van Duyne, *Appl. Spectrosc.*, **2007**, *61*, 994.

[49] P. Hildebrandt, M.J. Stockburger, *Phys. Chem.*, **1984**, *88*, 5935.

[50] B.L. Darby, E.C. Le Ru, *J. Am. Chem. Soc.*, **2014**, *136*, 10965.

[51] J.E. Selwyn, J.I. Steinfeld, *J. Phys. Chem.*, **1972**, *76*, 762.

Graphical Abstract - TOC

The different mechanisms involved in the molecule to SERS substrate interaction occurring even for structurally similar molecules strongly limit the possible qualitative/quantitative analysis of simple dye mixtures. Problems arising in SERS quantitative analysis of comparable anionic or cationic dyes are discussed.

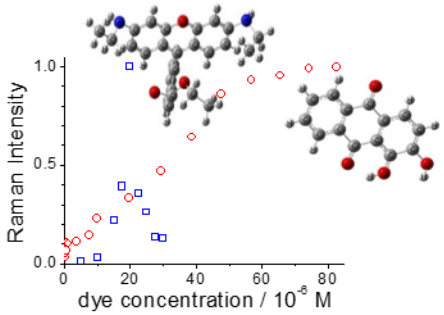

Supplementary materials

In Figure S1 (left) we show the extinctions spectrum of the colloidal dispersion before and after the mixing with pH 8 phosphate buffer solution. A strong aggregation of the AgNPs is suggested by the drastic reduction (much larger than the simple dilution factor) of the 415 nm peak, and the simultaneous increase of the optical extinction in the long wavelength region. In Figure S1 (right) the temporal stability of the native AgNPs colloid is shown as determined by the measure of different parameters of its extinction spectrum (wavelength and absorbance on the peak, and FWHM of the plasmonic band).

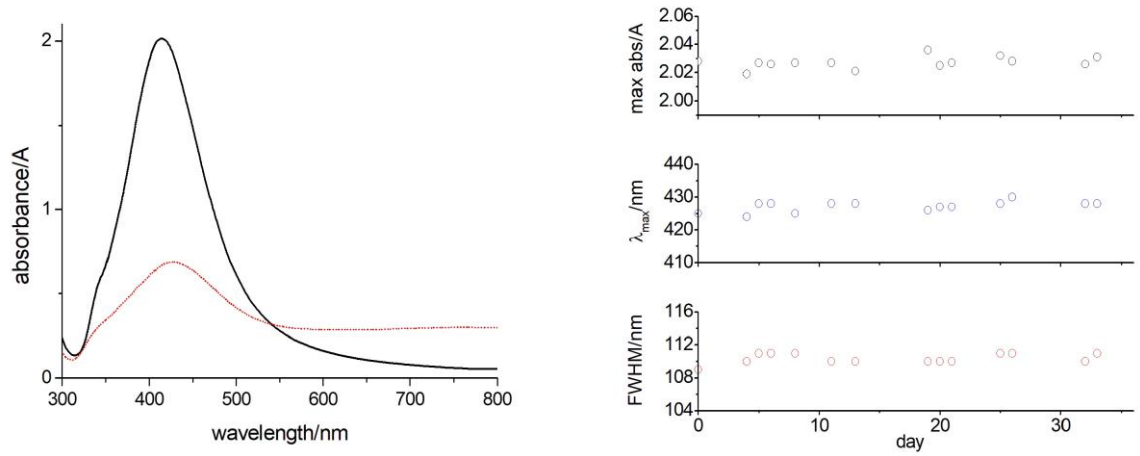

Figure S1. Properties of the AgNPs colloidal dispersion. Left: the extinctions spectrum (2 mm optical path) before and after the mixing with phosphate buffer solution at pH 8. Right: its temporal stability as determined through different parameters of the extinction spectrum (wavelength and absorbance on the peak, and FWHM of the plasmonic band).